Available online at www.sciencedirect.com
ScienceDirect
C. R. Physique 7 (2006) 959–976
COMPTES RENDUS PHYSIQUE
http://france.elsevier.com/direct/COMREN/

Nucleation/Nucléation

Nucleation problems in metallurgy of the solid state: recent developments and open questions

Yves Bréchet [a,*], Georges Martin [b]

[a] *LTPCM, domaine universitaire de Grenoble, 38402 Saint Martin d'Heres cedex, France*
[b] *CEA-Siège, cabinet du haut-commissaire, 91191 Gif sur Yvette cedex, France*

Available online 28 November 2006

Abstract

Nucleation processes play a key role in the microstructure evolution of metallic alloys during thermomechanical treatments. These processes can involve phase transformations (such as precipitation) and structural instabilities (such as recrystallisation). Although the word 'nucleation' is used in both cases, the situation is profoundly different for precipitation and for recrystallisation on which this article is focussed. In the case of precipitation, species are conserved and the underlying physics is stochastic fluctuations, allowing the apparition of critical germs of the new phase. In the case of recrystallisation, the underlying physical phenomenon is the progressive growth of subgrain structures leading to an unstable configuration, allowing a dislocation free grain to grow at the expense of a dislocated one. The two cases require different types of modelling which are presented in the article. ***To cite this article: Y. Bréchet, G. Martin, C. R. Physique 7 (2006).***
© 2006 Académie des sciences. Published by Elsevier Masson SAS. All rights reserved.

Résumé

Problèmes de germination dans de la métallurgie de l'état solide : des développements récents et des questions ouvertes. Les processus de germination jouent un rôle central dans les évolutions microstructurales des métaux et alliages observées au cours des traitements thermomécaniques. Ces processus peuvent résulter de transformations de phase (comme dans le cas de la précipitation) ou d'instabilités des défauts structuraux (comme dans la recristallisation). Quoique le terme de germination soit indifféremment utilisé dans les deux cas, la situation est profondément différente. Dans le cas de la précipitation, les espèces sont conservées, et la germination résulte de fluctuations statistiques autorisant l'apparition d'un germe critique de la nouvelle phase. Dans le cas de la recristallisation, le phénomène physique sous jacent est la croissance progressive d'une structure de sous grains, jusqu'à une configuration instable permettant la croissance d'un grain libre de dislocation dans une matrice fortement disloquée. Les deux cas nécessitent des traitements théoriques de nature différente qui sont présentés dans l'article. ***Pour citer cet article : Y. Bréchet, G. Martin, C. R. Physique 7 (2006).***
© 2006 Académie des sciences. Published by Elsevier Masson SAS. All rights reserved.

Keywords: Coherent precipitation; Recrystallisation
Mots-clés : Précipitation cohérente ; Recristallisation

* Corresponding author.
E-mail address: ybrechet@ltpcm.inpg.fr (Y. Bréchet).

1631-0705/$ – see front matter © 2006 Académie des sciences. Published by Elsevier Masson SAS. All rights reserved.
doi:10.1016/j.crhy.2006.10.014

1. Introduction: set the scene and the actors

Nucleation problems are ubiquitous in physical metallurgy, as long as they are understood as the initial step in a transformation process of the microstructure. They range from phase transformations occurring when an alloy is prepared in a state away from equilibrium (e.g. when a metal is quenched in a one phase state within a region of the phase diagram where its equilibrium state would be two phased), to the initial damage mechanisms when a particle undergoes decohesion or fracture under an imposed deformation of the component. These processes are both crucial to design alloy composition and thermomechanical treatments for optimal in use properties [1]. They are also among the fundamental questions still pending in the field. In the spirit of this issue, it is out of question to have even a brief overview of the variety of questions subsumed under the generic term 'nucleation': this would imply having to consider solidification, phase transformation, microstructure development during thermomechanical treatments, fracture in monotonic and cyclic loading, pitting corrosion, as examples of the variety of phenomena hiding behind the word 'nucleation'. Our purpose here is to limit ourselves to two nucleation processes, very different in nature, and amenable to very different theoretical treatments, which can be seen as representative of two different 'styles' of physical metallurgy. These two examples will be dealing with microstructural evolution in the solid state.

The first example deals with the simplest possible case of phase transformation: coherent precipitation. The driving forces here are clearly identified (from thermodynamic data) and the mobility elementary events are also well identified at the atomistic level: diffusion. The theoretical tools used to understand quantitatively the process are somewhat reminiscent of statistical physics which incorporates, as far as it can be done, the atomistic processes associated with atom mobility, in order to have the best possible description of the kinetic path. The ultimate goal is to have a description of the process with no adjustable parameters.

The second example deals with an other example of nucleation in microstructure evolution: recrystallisation. It exemplifies the other extreme, where the actors of the nucleation process are out of equilibrium defects which are non conservative, strongly interacting, and whose behaviour cannot possibly be described, without loosing an essential part of the physics, via the minimisation of a potential function. The tools used in this kind of problems are much more of a craftsman's art, back of the envelope calculations. The reasonable goal of the exercise is to provide a rationalisation of the observed phenomena, made quantitative with a limited number of adjustable parameters whose physical significance and order of magnitude are clearly identified.

2. An example from phase transformation

2.1. The simplest possible nucleation problem

The metallurgy of phase transformations offers a broad spectrum of nucleation problems, with a large range of complexity and a very diverse level of understanding. *Coherent precipitation*, i.e. the formation of solute clusters on the very same atomic lattice as the solid solution they grow from, is the simplest problem we may think of. It is rather common: Guinier Preaston zones (GPZ) formation in 'light alloys' (e.g. FCC Zn precipitates out of Al(Zn)), BCC Cu precipitates out of BCC Fe(Cu), as occurs in certain pressure vessel steels of nuclear reactors [2], A_3B precipitation with $L1_2$ structures out of FCC A(B) solid solutions: Ni_3X with $X = Al, Si, Ge, W$ or a mixture of Al with other elements is the family of 'nickel base super alloys' of broad use in high temperature aircraft engine industry [3]; Al_3X, with $X = Li, Sc, Zr, \ldots$ is a family of advanced light alloys for aircraft industry [4]. Notice that 'coherency' is more restrictive than 'epitaxy': coherent precipitates are epitaxial to the solid solution (common crystallographic orientations), but the lattice planes are continuous through the precipitates: as a result, the interfacial energy is weak, typically $\approx 10\ \mathrm{mJ\,m^{-2}}$. Most generally, fully coherent precipitates induce a lattice strain (which increases with the volume of the precipitate), but the latter may be very small, because of a very small lattice mismatch between the precipitate and the matrix; the coherency strain can then be safely neglected, at least in the early stages of the precipitation process: such is the case in Fe(Cu), or in some super alloys. In the following, we restrict ourselves to the last most simple case of coherent precipitation with negligible associated coherency strain. Notice also that coherent precipitation occurs both in solid solutions with a very low solute solubility (0.1 at% and less) such as Fe(Cu), Al(Zr, Sc), or with large solubility ($\approx$10 at% and more) such as Al(Li), Ni(Al, ...).

At the atomic scale, coherent precipitation with negligible associated coherency strain, is nothing but thermally activated atomic jumps on a lattice: solute atoms change lattice sites by jumping into a nearest neighbour vacant

site. As a result, solute clusters form and evaporate. Depending on the solute content of the matrix and on the jump frequency spectrum of the solute (the jump frequency depends on the local atomic configuration close to the vacancy), clusters will grow or shrink: phase separation will eventually result. Such a simple process is the crystalline counterpart of nucleation in a gas or in a fluid, such as the condensation of water out of air, or evaporation of air out of liquid water. However, since the description of diffusion at the atomic level is more precise in crystals than in fluids [5,6], and since solids can be observed at the atomic scale at various stages of decomposition (owing to atom probe field ion microscopy, or atom probe tomography, APT [7]), metallurgy has promoted during the past decade a renewed understanding of nucleation and of the classical theory thereof. Such progress is based on a combined use of atomic resolution observations (APT), atomic scale modelling of atomic diffusion based on Kinetic Monte Carlo techniques (KMC), and of classical models (cluster dynamics and nucleation theory). One important result is the clarification of the impact of the diffusion mechanism on the kinetic pathway[1] for phase separation. Among interesting results, the proper choice of the diffusion coefficient to enter the classical theory resolves the long standing controversy on the quantitative agreement between theory and experiment, at least in the simple case of strain free coherent precipitation. Also unique features of the impact of the details of the diffusion mechanism on the kinetic pathway for phase separation have been revealed and explained.

2.2. *Nucleation of coherent precipitates*

Coherent precipitation can be observed at all scales down to the atomic scale, either in real space (APT, Transmission electron microscopy—TEM) or in Fourier space (small angle neutron or X ray scattering—SANX/S). It can be modelled by the classical nucleation theory (CNT), or by cluster dynamics (CD), which both yield to particle size distribution as a function of time. However, during the last decade, technical improvements made it possible to observe and to model *at the atomic scale*, similar volumes of matter ($\approx 20 \times 20 \times 100\ \mathrm{nm}^3$ and more). The modelling is based on KMC simulations of the diffusion of a vacancy in a solid solution. One important recent result is the convergence of all the available techniques, both experimental and modelling ones, provided some care is taken.

2.2.1. *Observation and modelling techniques give a single consistent picture of nucleation*

Numerous studies of precipitation are available. In some rare cases, the full spectrum of observation and modelling techniques has been applied on the very same alloy: such is the case for $\mathrm{Al}(\mathrm{Sc}_x, \mathrm{Zr}_{(1-x)})$[2] which presents an interesting decomposition pathway and which has been extensively studied using small angle scattering techniques, high resolution electron microscopy, tomographic atom probe, kinetic Monte Carlo simulations and cluster dynamics modelling [9]. The main results can be summarized as follows:

- A supersaturated solid solution of zirconium and scandium in aluminium (both elements have a very low solubility) decomposes by forming Al_3X ($X = \mathrm{Sc}$ or Zr) precipitates, fully coherent with the matrix: such precipitates are a superstructure of the underlying FCC aluminium lattice, with Al atoms at the centre of the cube faces, and X at the apex of the cube ($\mathrm{L1}_2$ structure);
- All the observation techniques used (see above) converge to the same fine scale structure of the precipitates: a Sc rich core surrounded by a Zr rich shell;
- KMC simulations of the diffusion of one vacancy in a model $\mathrm{Al}(\mathrm{Sc}, \mathrm{Zr})$ solid solution, once carefully parameterised[3] lead to the formation of $\mathrm{L1}_2$ precipitates with the same 'core shell' structure as observed experimentally. It is worth mentioning that the KMC simulations were achieved before the experimental observations had been done!

[1] A 'kinetic pathway' is the succession, parameterised in time, of the morphologies the alloy goes through.

[2] Work supported by a coordinated research program lead by CNRS, with ARCELOR, ALCAN and CEA ("CPR Precipitation") [8],

[3] For the details of the technique and of the parametrisation procedure, see [9]. The KMC simulation of vacancy diffusion in an alloy implies configurational energies both for the stable and for the saddle point configurations. The former are deduced from a cluster expansion of the results of first principle calculations (DFT-LDA); the latter imply a binding energy at the saddle point, which is empirically fitted to experimental tracer diffusion data.

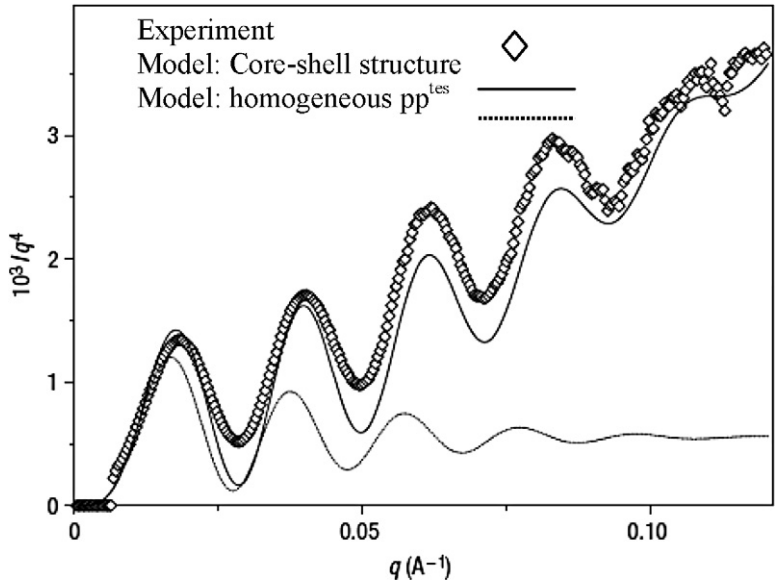

(a)

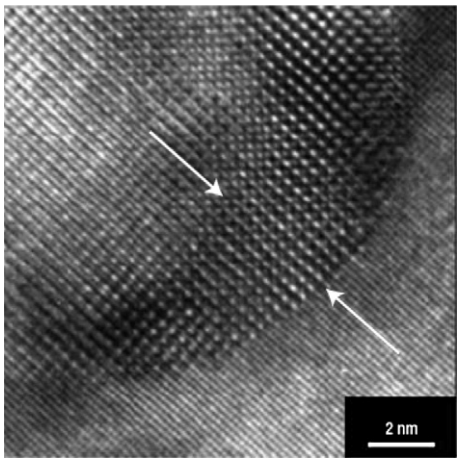

(b)

Fig. 1. The core-shell structure of $Al_3(Sc, Zr)$ precipitates is revealed by all the observation techniques used so far ((a) SAXS, (b) High resolution TEM, (c) APT) and (d) comes out of the KMC simulations as well (courtesy of respectively Dr. A. Deschamps, Prs. T. Épicier & D. Blavette, and Dr. E. Clouet).

KMC then reveals the origin of the core-shell structure of the precipitates. Scandium is known to diffuse much faster than zirconium in aluminium, hence there is no surprise that scandium atoms cluster first, and zirconium reaches the latter clusters later. Once zirconium has reached the scandium rich clusters, it is trapped at the periphery because of the vacancy diffusion mechanism, which prevails in the A_3B compound: the interdiffusion of Zr and Sc is very slow, since the process implies the formation of energetically unfavourable anti-site defects (Zr or Sc on the Al sublattice). Even though the vacancy jump frequency in A_3B might be large, the diffusion on the B sublattice is very slow because of *strong kinetic correlations* (see Fig. 1).

Beyond qualitative arguments as above, more quantitative studies have also revealed interesting features of the nucleation process.

2.2.2. Some theoretical issues

Since KMC simulations of the diffusion of one vacancy in a solid solution well reproduces what is actually observed, the technique may be used to address some theoretical questions.

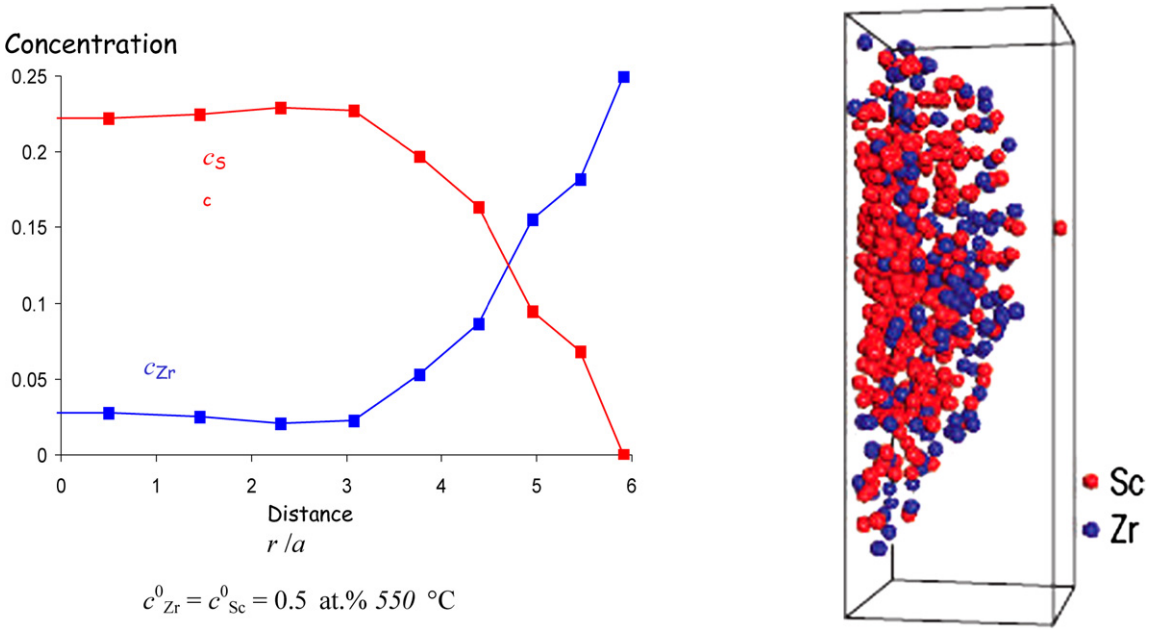

(c)

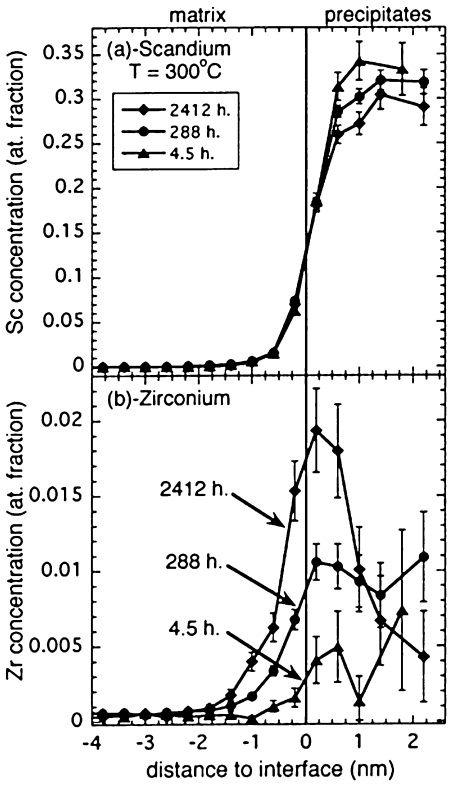

(d) APT concentration profiles at $Al_3(Sc, Zr)$ precipitates (courtesy of Pr. D. Seidman) B. Fuller, D. Seidman, Acta Mater. 53 (2005) 5415

Fig. 1. (*Continued*.)

2.2.2.1. Quantitative assessment of the nucleation theory. In alloys with low solubility limit, provided the solid solution is dilute enough to prevent solute percolation, solute clusters may be defined unambiguously and the classical nucleation theory can be given a very transparent form [10]: the alloy can be described as a lattice gas of solute clusters,

the size distribution of which, C_n, is governed by a master equation. The latter becomes very simple whenever the migration of solute clusters may be neglected; in this particular case, single particle events only, do contribute to the transition probabilities:

$$\frac{\partial C_n}{\partial t} = J_{n-1,n} - J_{n,n+1}; \quad J_{n,n+1} = \beta_{n,n+1} C_n - \alpha_{n+1,n} C_{n+1}$$

With the above restrictive hypothesis, the condensation rates, $\beta_{n,n+1}$ are usually written as:

$$\beta_{n,n+1} = 4\pi D_1 C_1 R_n \Omega^{-1}$$

C_1 and D_1 are respectively the concentration and the diffusion coefficient of isolated solute atoms (monomers); D_1 is named the 'impurity diffusion coefficient' in the metallurgical literature. R_n is the capture radius of a cluster of size n. As for the evaporation rate, $\alpha_{n+1,n}$, the latter is assumed to be a characteristic of the cluster, independent of the gas of clusters it is embedded in. The values of the evaporation rates can therefore be estimated from any equilibrium state, taking advantage of detailed balance:

$$\alpha_{n+1,n} = \overline{\beta}_{n,n+1} \overline{C}_n / \overline{C}_{n+1}$$

Over-lined quantities are given their equilibrium value. Without going into details, it is clear that the ratio $\overline{C}_n/\overline{C}_{n+1}$ implies the size dependence of the interfacial contribution to the cluster free energy ($2\sigma\Omega/R_n kT$ for a macroscopic sphere, with σ for the interfacial energy).

That such a formalism is reasonable has been assessed quantitatively by a combined use of TAP, KMC simulation of the diffusion of one vacancy and cluster dynamics based on the same set of parameters as the KMC simulations [11]. The work was performed on the same alloys as above, but in binaries ($x = 0$ or $x = 1$), using the same procedure to parameterize the KMC model. The free parameters entering Cluster Dynamics are, D_1 and σ. The impurity diffusion coefficient is 'measured' on KMC simulations (and is found in good agreement with the known experimental value): it is verified that solute complexes do not migrate, which makes the system suitable for being described by the above master equation. The interfacial free energy, σ, is computed from the interatomic pair interactions, exactly for the smaller clusters (up to $n = 9$) and then extrapolated to its macroscopic mean field value. A (negative) curvature correction is found (as expected). Since the cluster is a crystalline one, the size dependence of σ, is better understood in terms of the sum of three contributions: that of faces, of edges and of apexes which go respectively as $n^{2/3}$, $n^{1/3}$, n^0 [12]. Once so parameterized, numerical integration of the master equation yields the cluster size distribution as a function of time, from which the time evolution of the mean cluster size is deduced.

Two important results are found; they are illustrated on Fig. 2:

- Cluster dynamics well reproduce the KMC results, as far as the mean cluster radius is concerned. At variance with what has often been claimed,[4] there is no gross quantitative discrepancy between the theory of nucleation, as used here, and the atomistic simulation of nucleation;
- Once the above agreement is established, the master equation can be integrated up to n times, which are several orders of magnitude larger than the times achieved by the KMC simulations. The mean radius so computed is found to be within the scatter of existing experimental observations. Notice that the latter were not used to parameterize the KMC.

Despite this success, some points remain to be clarified: in particular, the cluster *size distributions* as computed by CD and as determined from KMC simulations do differ slightly (although with very similar mean radii). Lepinoux correctly argues that for the smaller clusters, since the specific interfacial energy, σ, implies face, edge and apex contributions, the capture radius R_n, should do as well: $R_n = R_0 + R_1 n^{1/6} + R_2 n^{1/3}$ [13].

2.2.2.2. Impact of the diffusion mechanism on the decomposition pathway. The intensive use of KMC to simulate vacancy diffusion in supersaturated alloys, with nucleation, growth and coarsening as a result, has revealed that details of vacancy diffusion may deeply affect the kinetic pathway for phase separation. Indeed, it is a simple matter to modify

[4] A discrepancy by more than 10 orders of magnitudes is sometimes announced.

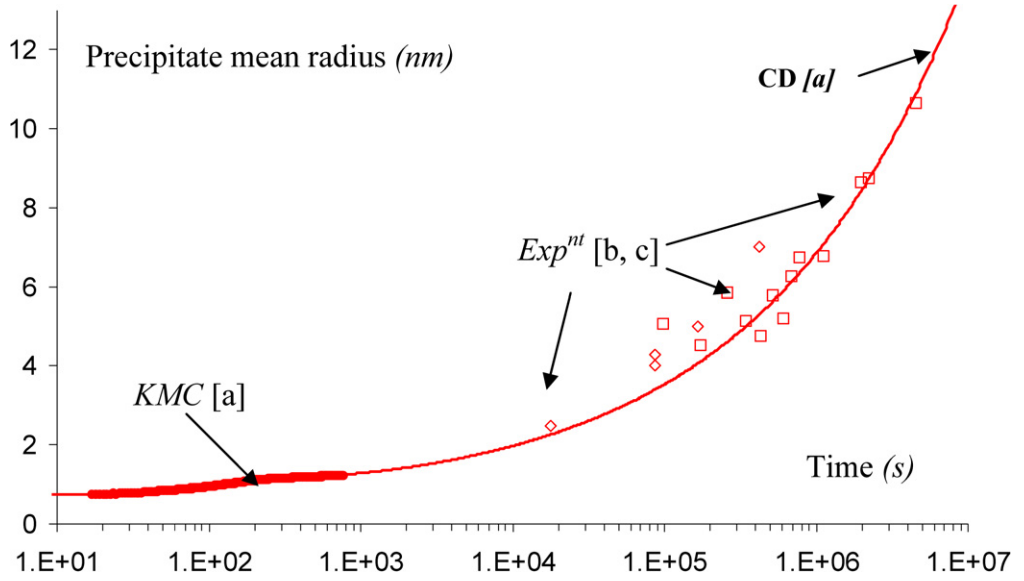

Fig. 2. Cluster Dynamics, once properly parameterized, well reproduces the mean precipitate radius obtained from KMC simulations as well as the existing experimental observations *at much larger times*. (Courtesy of Dr. E. Clouet.) (a) E. Clouet et al. [11]; (b) G.M. Novotny, A.J. Ardell, Mater. Sci. Eng. A 318 (2001) 144–154; (c) E. Marquis, D. Seidman, Acta Mater. 49 (2001) 1909.

the parameters entering the KMC simulation, in such a way as to modify the kinetic correlation effects in diffusion,[5] keeping the driving force for nucleation the same.

The first example is given by Soisson et al., in the case of *dilute alloys* [14,15]. Soisson first recognised that the (local) concentration dependence of the saddle point energy for vacancy jumps plays a significant role on correlation effects: depending on the latter dependence, solute clusters may or may not contribute to solute diffusion, and if they do contribute, their migration is more or less correlated. A spectacular result concerns the case of weak solute supersaturation, i.e. of high nucleation barriers: whenever solute clusters do not contribute to solute diffusion, KMC well reproduces an incubation period followed by nucleation, then growth and finally coarsening. Keeping the thermodynamics the same and allowing for cluster migration erases the nucleation stage. The solid solution behaves as an unstable one, with no nucleation stage left. A qualitative explanation is that, because of the migration of small clusters, the size of a nucleus may achieve large jumps, i.e. 'diffuse' more rapidly across the nucleation barrier. The specific case of a model Fe(Cu), has been studied in detail. Semi-empirical potentials [15], as well as first principle calculations [17], yield saddle point configuration energies as a function of the composition in the first neighbour shell of the saddle point. The composition dependence is distinct for Fe and Cu. Small variations of the latter dependence modify the correlation among successive jumps of small solute clusters, with important modification of the nucleation rate (see also [18,19]).

In mutlicomponent *concentrated* alloys also, the correlation effects in diffusion have been demonstrated to affect the early stage morphology of phase separation. Blavette and co-workers were the first to demonstrate that the early stages of phase separation, as observed by APT and TEM, in a concentrated ternary alloy, Ni(Al, Cr),[6] could be well reproduced by KMC simulations of the diffusion of one vacancy in a properly parameterised model alloy [20]. This study has recently been extended by Seidman and coworkers [21]. In this latter work, an interesting feature observed both in ATP and KMC, is the occurrence, during the nucleation and early growth stages, of many coagulated

[5] The origin of kinetic correlation effects can be summarized as follows. Because an atom can only jump to a vacant lattice site, the probability for an atom to jump in one of the Z nearest neighbour directions is not merely given by the energy landscape: it is non zero only for that direction which points to the vacancy. The probability for the vacancy to occupy one specific neighbour site of the atom at a time t is correlated to its previous occupancy of that site: indeed, many jumps sequences of the vacancy will bring the latter back to the site it started from. As a result, the successive jumps of a given *atom* are correlated in time. While such effects have been clarified in the early 1940s for a one component system, concentrated non ideal alloys still deserve active research [6,16].

[6] The Al and Cr contents were respectively 5.2 and 14.7 at%, aging was performed at 873 K for time ranging from few minutes to hours.

precipitates, i.e. nearby precipitates, which are connected by a neck; the latter tend to disappear during the coalescence stage. Since the solid solution is concentrated, and the range of interatomic pair interactions is known to extend to the fourth neighbour, solute clusters can no longer be defined unambiguously. We rather define concentration fields around precipitates, by averaging over several precipitates of similar sizes the concentration on neighbouring sites. The time evolution of the latter concentration fields is governed by the diffusion equation, the coefficient of which (i.e. the elements of the diffusion matrix) can be evaluated from KMC simulations in the equilibrium terminal solid solution.[7] Doing so, we demonstrate that the coagulation process is due to broad diffusion profiles around the precipitates, much broader than an equilibrium interfacial thickness; the anomalous width of the former is the result of *kinetic* correlations among the fluxes. By cancelling the long range solute vacancy binding, in the KMC parameters, it is possible to annihilate the latter correlations, without altering the thermodynamics of the alloy: the concentration profiles around

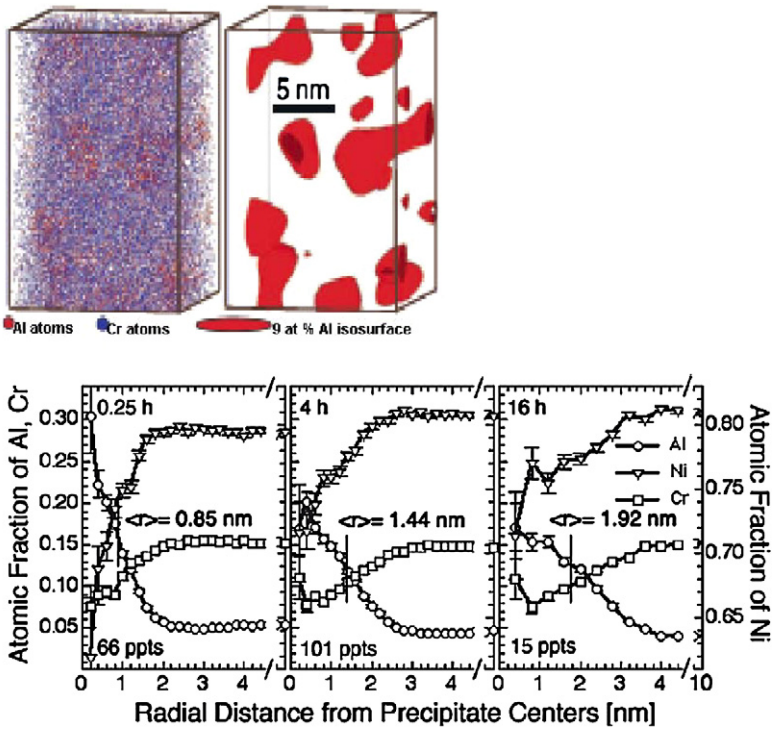

Fig. 3. Coagulated $Ni_3(Cr, Al)$ precipitates revealed by APT in Ni(Cr, Al) alloys (left) and an Al iso-concentration surface to visualize the precipitates. Below, Ni, Cr, Al, concentration profiles deduced from APT studies, by averaging over several precipitates; notice the width of the transition region between the precipitate (to the left) and the matrix (to the right), much larger than an equilibrium interfacial layer; increasing aging times, at 600 °C are shown (courtesy of Pr. D. Seidman).

[7] In a multicomponent solution, with S chemical species, which diffuse on a lattice via vacancy jumps, the flux $\tilde{J}$, a vector of components J_i ($i = 1$ to S) is a linear combination of the driving forces, i.e. of the *gradient of chemical potentials* relative to the vacancy ($\mu_i - \mu_v$): $\tilde{J} = -\overline{\overline{L}}\nabla\tilde{\mu}(\Omega kT)^{-1}$, with $\tilde{\mu}$, the vector with components ($\mu_i - \mu_v$). $\overline{\overline{L}}$ is Onsager's matrix, Ω the atomic volume; the diffusion matrix, relates the same diffusion flux to the *concentration gradients* (relative to vacancies $C_i - C_v$): $\tilde{J} = -\overline{\overline{D}}\nabla\tilde{C}\Omega^{-1}$. The two matrices are related by the susceptibility matrix, the Jacobian of the free energy function with respect to the concentrations:

$$\overline{\overline{D}} = -\overline{\overline{\chi}}\,\overline{\overline{L}}(kT)^{-1}; \quad \chi_{ij} = \frac{\partial(\mu_i - \mu_v)}{\partial C_i} = \frac{\partial^2 F}{\partial C_i \partial C_j}$$

The off diagonal terms of Onsager's matrix reveal kinetic correlations among the fluxes, while those of the susceptibility matrix reveal the full composition dependence of each of the chemical potentials. The off diagonal terms of the diffusion matrix combine the two latter effects. The elements of Onsager's matrix can be computed from the spectrum of the exchange frequency of a vacancy with its neighbour (as a function of the vacancy surrounding), based on various mean field kinetic theories; they can also be evaluated, from kinetic Monte Carlo simulations, based on the same frequency spectrum, using the fluctuation dissipation theorem [5,6]. The susceptibility matrix can be evaluated by standard equilibrium Monte Carlo techniques.

the precipitates sharpen and the necking process does not show up any longer; coalescence proceeds via the standard evaporation condensation mechanism [22] (see Fig. 3).

2.3. Conclusion

Coherent precipitation with negligible coherency strain is not uncommon is real metallic alloys. As all first order transitions do, these exhibit nucleation, growth and coarsening stages, which result from nothing but successive jumps of a vacancy on the lattice. This extreme simplicity allows clarifying long-standing issues in the theory of nucleation, taking advantage of a combined use of atomic scale *observation* and *modelling* techniques. It is shown that the classical theory of nucleation, when applicable in its cluster dynamics version, yields an excellent quantitative agreement (better than one order of magnitude) with the experimental observations; more over, for a given nucleation barrier, the kinetic pathway of phase separation is shown to be strongly influenced by details of the diffusion mechanism: in low solubility alloys, fast migration of small clusters may suppress the incubation period; in concentrated alloys, kinetic correlations among fluxes (which is reflected in the off diagonal terms of the Onsager's matrix) affect the interfacial width of precipitates at early stages and may trigger necking between nearby precipitates. We believe that many more effects of this sort remain to be explored and that the above clarifications should have some consequences on the understanding of more complex nucleation processes in solids.

3. Nucleation process in recrystallisation

3.1. Annealing of deformed structures

When deformed plastically, most metallic alloys store structural defects responsible for plastic flow, namely dislocations [23]. These defects are very costly from an energetic viewpoint (the line energy is of the order Gb^2 where G is the shear modulus and b the lattice parameter), and this internal energy cannot be paid for by an entropic term, so these defects are out of thermodynamic equilibrium. The only reason for which dislocations remain in the material is that the solid friction opposes their motion, and the strong interaction between dislocations tends to create efficient obstacles to their motion (this fact is responsible for the increased hardness of a deformed material known as work hardening). Dislocations are linear defects with long range interactions, and they are not conservative: during plastic flow they can annihilate or multiply, but there is nothing like an equilibrium density of dislocations. These defects carry an elastic field and interact with each other. They can also interact via short range reactions involving the core of the defect where crystallographic order is most perturbed. The result of these complex interactions is a self organisation of dislocations into subgrains, whose size scales as the inverse of the flow stress under which plastic flow is imposed [1]. The reason why this spontaneous patterning occurs is still an open question, but this patterning plays a key role in the subsequent annealing processes [24].

When the material is annealed post deformation, dislocations acquire an increased mobility and the system tends to decrease its free energy by getting rid of stored dislocations. This process softens the material and can take place, depending on the initial defect density and on the annealing temperature, in several ways, either homogeneously and progressively, or heterogeneously and rapidly.

The process by which dislocations disappear progressively, relaxing the internal stresses in a collective and roughly homogeneous process, is known as recovery. It leaves the crystallographic texture of the material basically unchanged, and the granular structure is also conserved. This process is slow and follows a kinetic logarithmic in time. It occurs for ranges of predeformations rather small and annealing temperatures relatively low. It is progressive and does not seem to require an incubation time to appear.

By contrast, the recrystallisation process is much faster, and resembles a nucleation/growth process. The overall kinetics of recrystallization appears to be amenable to a nucleation and growth treatment. In fact, the classical Johnson–Mehl–Avrami description of a nucleation and growth reaction was initially developed to describe the recrystallization of aluminum [25]. During recrystallisation, regions of the material 'nucleates' new grains, free of dislocations. These grains, deprived of dislocations, have a lower free energy, and they grow at the expense of the surrounding regions; the decrease in dislocation density is much faster, much more heterogeneous and occurs via the creation of some new grains, free from dislocations, which grow at the expense of the regions of the materials in which dislocation are still present. This process is heterogeneous (it takes place at special locations in the alloy, at

grain boundaries, at particles, at shear bands...). It profoundly modifies the crystallographic texture of the material and its granular structure. It involves a 'nucleation step' requiring an incubation time.

In general, recovery dominates at low annealing temperatures whereas recrystallization is favored at higher temperatures [24]. It should be emphasized, however, that the two processes are not exclusive. In fact, recovery takes place during the incubation time preceding nucleation and continues to operate even after the onset of recrystallization. As such, recovery and recrystallization may coexist and compete with each other [26,27].

It is generally accepted [24] that the mechanism of recrystallization must involve a nucleation step during which a new grain, free of dislocations, appears. At first sight, the nucleation step of recrystallization may seem reminiscent of nucleation in phase transformations, where the surface energy increase due to the creation of an embryo is balanced by the decrease in bulk free energy during the transformation. It has been shown, however, that the size of the new grains (which could be of the order of several microns) is physically inconsistent with any classical nucleation model involving a fluctuation process [24]. The macroscopic consequences of the existence of a nucleation step are very important from the viewpoint of microstructure control. In fact the 'fundamental laws of recrystallization' [24] may be largely interpreted in terms of the nucleation step. These laws state that recrystallization takes place only when the initial strain is above a threshold known as the 'critical strain'. When the material is deformed beyond this critical strain, recrystallization takes place after a given nucleation/incubation time. Both the critical strain and the incubation time decrease with increasing annealing temperature. Alternatively, for a given strain, recrystallization will take place only above a critical annealing temperature known as the 'recrystallization temperature', and this critical temperature is lower if the initial strain is higher.

3.2. Nucleation of recrystallisation as a structural instability

An alternative approach to the 'classical nucleation theory' was proposed by Bailey and Hirsch [28], in which, the nucleation step is interpreted as an instability of the microstructure, rather than a fluctuation at the atomic scale. The general picture proposed by Hirsh is that the recovery of dislocations close to an interface of high mobility (such as a grain boundary or a dislocation wall developing close to a non deformable particle) leads to the 'bowing out' of this interface when the decrease in energy provided by this expansion of the 'dislocation free zone' can pay for the energy cost of expanding the interface. This simple and elegant idea leads naturally to define a length scale L for this instability, namely the ratio of the surface energy γ to the stored energy per unit volume G. When the zone where recovery exceeds this size, bowing out can take place. The Bailey–Hirsh criterion is the exact equivalent of the criterion for operating a Frank Read source to nucleate dislocations above a critical threshold stress. An extra complexity stems, however, from the fact that, during the incubation time leading to the fulfillment of Bailey–Hirsh criterion, recovery take place, resulting in a decrease of the driving force G, and therefore to an increase of the critical length L. From this simple idea, we can provide a predictive physically-based model for the nucleation of recrystallization. The inputs of the model are well-defined and measurable quantities such as the recovery kinetics, the grain-boundary mobility and initial subgrain size. The model outputs include the incubation time, critical strain and critical temperature for recrystallization as well as the nucleation rate. Ultimately, a complete description of the evolution of the recrystallized fraction with time could be obtained by coupling the present model to a growth model.

Two main ideas are at the heart of the present model [29], namely, that:

(a) nucleation must be analyzed as a microstructural instability of the subgrain structure rather than a fluctuation phenomenon [30];
(b) there exists an interplay between recovery and recrystallization.

Starting with the first concept, a nucleus is formed when the subgrain/cell size, r, increases beyond the value at which the curvature force, $2\gamma/r$, just balances the driving force for recrystallization, G. Mathematically, this is identical to the Bailey–Hirsch nucleation criterion:

$$r(t) > r_c(t) = \frac{2\gamma}{G(t)}$$

where r_c is the radius that a subgrain needs to reach in order to become a viable nucleus and γ is the grain boundary energy.

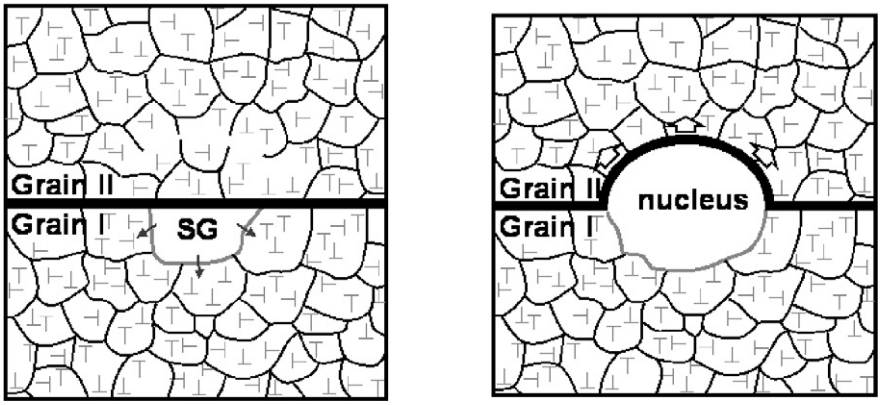

Fig. 4. Schematic of the 'Bulging Mechanism' for nucleation of recrystallisation.

The above nucleation criterion could be visualized in terms of the recrystallization nuclei shown in Fig 4. In this example, nucleation was assumed to take place in the vicinity of a high angle grain boundary. Subgrain growth occurs as a consequence of the recovery process. The capillary term, $2\gamma/r(t)$, gradually decreases as subgrain growth progresses. When the capillary term drops below the instantaneous value of the stored energy, $G(t)$, the subgrain will 'bulge' into the neighboring grain, as shown in Fig. 4, and a nucleus is said to be formed. This nucleus will preferentially grow into the neighboring grain because it benefits from a very mobile high angle boundary. This process is known as strain-induced boundary migration (SIBM) and is expected to dominate at small and medium strains. Other nucleation processes such as particle stimulated nucleation, PSN, and nucleation in shear bands, could, in principle, be described using the framework of the present model. Their occurrence reflects the necessity to have both stored energy and highly mobile interfaces to provide efficient nucleation sites.

We next turn our attention to the second key concept of the interaction between recovery and recrystallization. Recovery both provides a mechanism for subgrain growth, but also a process to decrease the stored energy. In that sense, it is both necessary, and competing with recrystallisation nucleation. The decrease of the stored energy, $G(t)$ has the consequence that the size of the critical nucleus, $2\gamma/G(t)$, will increase with time. The occurrence of nucleation is then dependent on the competition between the rate at which the critical subgrain radius increases, and the rate at which a given subgrain (of mobility M) can grow to reach the critical size. This competition naturally leads to the concepts of the critical strain and critical temperature for recrystallization.

3.3. Nucleation criterion

The critical subgrain size, $r_c(t)$, represents the size above which a subgrain overcomes the capillary forces and starts to grow rapidly. The critical subgrain size, $2\gamma/G(t)$ increases as a result of the recovery of the global driving force, and the average subgrain size $r(t)$ increases due to the growth of a particular subgrain in response to its local environment, in order to reduce the total sub-boundary energy. This competition is illustrated in Fig. 5, where both r_c and r have been plotted as a function of time. The dotted lines in the above figures indicate the average subgrain size, $\langle r(t)\rangle$, and the shaded area reflects the fact that a range of subgrain sizes would exist in any given sample.

In Fig. 5(a), none of the subgrains present in the sample reaches the critical size and as such no recrystallization nuclei are formed. This would be the case, for example, when the initial strain is less than the critical strain or when the annealing temperature is less than the recrystallization temperature. In contrast, nucleation takes place for the cases illustrated in Fig. 5(b) which could be interpreted as corresponding to $\varepsilon > \varepsilon_c$ and $T > T_c$. The first nucleus is formed when the shaded area first touches the curve for r_c. This corresponds to the largest subgrain in the population reaching the critical size. With time, increasingly smaller grains will attain the critical size and more nuclei will be formed. Progressively, subgrains, which were initially too small, will reach the critical size. The nucleation rate may then be calculated if the subgrain size distribution and the number of nucleation sites are known.

In order to realize this program, one needs to evaluate the kinetics of subgrain growth and the rate of recovery. The detailed mechanisms of dislocation motion leading to cell and subgrain growth have been reviewed by a number of

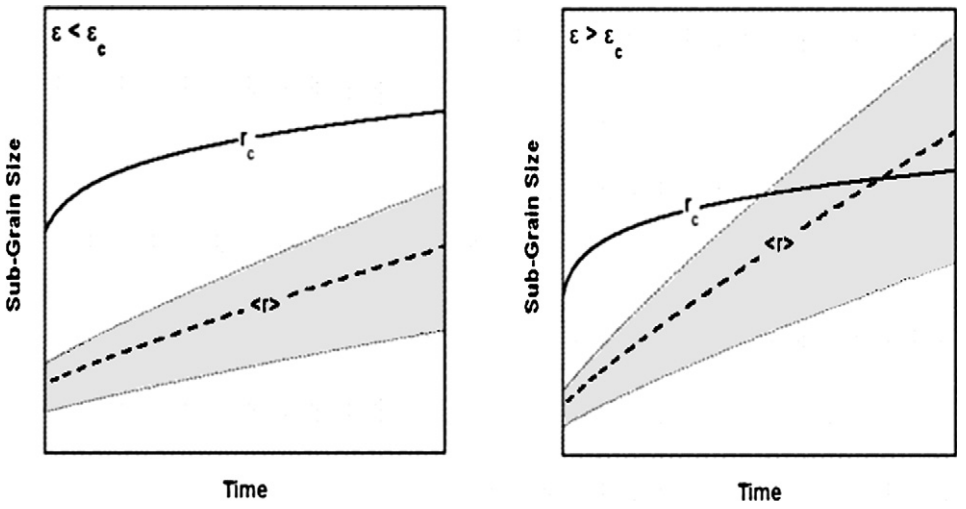

Fig. 5. Comparison of subgrain growth and critical subgrain size.

authors [24,31,32]. It is usually assumed that the rate of subgrain growth can be described using a simple law of the type:

$$v(t) = MG(t)$$

where v is the rate of subgrain growth and M is the sub-boundary mobility. The driving force used here, $G(t)$, is a global quantity which comprises both the dislocations in the subgrain boundaries and those in the subgrain interior. For a subgrain of initial size r_0, the size at time t is given by:

$$r(t) = r_0 + \int_0^t MG(t)\,\mathrm{d}t$$

In the present treatment, it is assumed that the subgrain-size distribution remains self-similar during subgrain growth, which means that the distribution of the normalized subgrain size, $r(t)/\langle r(t)\rangle$, is invariant. As such, it is not necessary to follow the evolution of individual subgrains. Rather it is sufficient to monitor the evolution of the average subgrain size.

The recovery rate can be directly measured my hardness measurements. It can also be modeled as an internal relaxation phenomena which leads to a logarithmic time dependence [23,33].

For a subgrain of size $r(t) = \chi\langle r(t)\rangle$, the nucleation criterion may be expressed as a critical value of the normalized subgrain size, χ:

$$\chi > \chi_c = \frac{2\gamma}{G(\langle r_0\rangle + \int_0^t MG(t)\,\mathrm{d}t)} \tag{1}$$

The time evolution of χ_c is illustrated in Fig. 6. At short times the decrease in $G(t)$ controls the evolution of χ_c, while at longer times the increase in the average subgrain size is the dominant mechanism. Depending on the position of the maximum of χ_c with respect to the maximum normalized subgrain size (of order 2 or 3, the size distribution of subgrains being generally expressed as a Log normal distribution or as a Rayleigh distribution), the system will undergo only recovery, or will be able to nucleate new grains. Fig. 6 also shows the definition of the recrystallization incubation time. The incubation time corresponds to the time necessary for $\chi_c(t)$ to fall below the value of χ corresponding to the largest subgrain in the distribution, $\chi_{\max} = r_{\max}/\langle r\rangle$.

When the stored energy is sufficiently large, the value of χ_c will eventually drop to within the range of subgrain sizes present in the sample and nucleation will take place. The nucleation rate and the number of nuclei can be derived if the subgrain size distribution and the number of nucleation sites are known. Let $P(\chi)$ be the density function of the

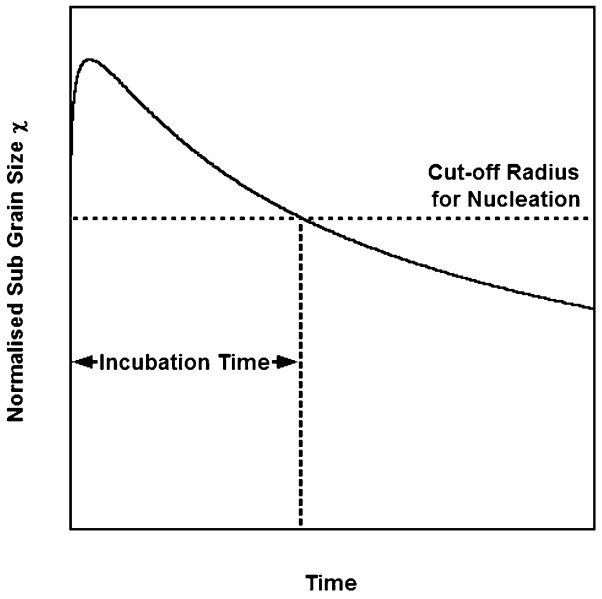

Fig. 6. Evolution of the normalized critical subgrain size χ_c.

subgrain size distribution, then the fraction of subgrains which would develop into recrystallization nuclei during an annealing treatment of duration, t, is given by:

$$f(t) = \int_{\chi_c(t)}^{\infty} P(\chi)\,\mathrm{d}\chi$$

As $\chi_c(t)$ decreases (due to subgrain growth) the fraction of subgrains which are able to form recrystallization nuclei increases. This fraction can be related to the actual number of nuclei if the type of nucleation sites is known. For example, when nucleation takes place on grain boundaries, it is reasonable to assume that the number of potential nucleation sites per unit volume is proportional to $1/(D\langle r\rangle^2)$, where D is the grain size. It is important to keep in mind that the nucleation rate obtained using the present model is not constant and will change with time. This trend is in agreement with the bulk of metallographic observations on the evolution of the number of recrystallized grains [24].

The simplicity of the present model conceals some subtle points which are of great importance. The first of these concerns the value of the sub-boundary mobility and the role of orientation gradients in the development of recrystallization nuclei. The mobility should be the mobility of the sub-boundary. There is reasonable evidence that the sub-boundary mobility could be expressed as a fraction of the high angle boundary mobility, M_{HAB} [34]:

$$M_{\mathrm{Sub}} = g(\theta) M_{\mathrm{HAB}}$$

where the factor g is a function of the sub-boundary misorientation, θ. Typically, $g(\theta)$ would vary between 0.005 for a small misorientation of 2.5° and 1 for a misorientation of 15° [34]. In a full treatment, the value of the mobility should be allowed to evolve as the misorientation builds up during annealing. In using a constant mobility, we are essentially using an average or an effective value. For all practical purposes this effective mobility should lie between $0.01 M_{\mathrm{HAB}}$ and M_{HAB}. Given the fact that accurate estimates of M_{HAB} are seldom available, the mobility term, M is best used as an adjustable parameter. In what follows, we will use the available experimental values of M_{HAB} as a starting point and adjust the factor $g(\theta)$ to obtain the best fit with the experimental data. The temperature dependence of the nucleation rate, however, is a consequence of the model, not an input.

The present discussion of the effective mobility brings us to the important role of orientation gradients in the nucleation of recrystallization [24]. When subgrain growth takes place within a strong orientation gradient, the effective value of M would be a large fraction of M_{HAB} and recrystallization would be expected to take place rapidly. At the other extreme, that is, in the absence of an orientation gradient, the effective mobility will be equal to the initial sub-boundary mobility. This is usually very small and as a result, the evolution of will be dominated by the recovery

term and recrystallization may not take place. The use of the effective mobility as an adjustable parameter is only meaningful when the deformed structure contains the orientation gradients necessary for nucleation.

Another limitation in the present approach is to limit the description of the subgrain structure to a description of its size distribution. A more consistent treatment would involve a description of the subgrain wall misorientation distributions.

3.4. Quantitative applications of the model

In spite of these many assumptions, the model can be used to describe quantitatively the nucleation of recrystallization in two classes of materials. The first class consists of small and medium stacking fault energy materials in which negligible recovery of the cold-rolled structure is observed prior to recrystallization [35]. The subgrain structure evolves, but the dislocations within the subgrains have a very slow recovery rate. In these materials the nucleation time is controlled almost completely by the sub-boundary mobility and its dependence on temperature. This class of materials is exemplified by oxygen-free Cu, for which a reasonable amount of information is available on the microstructure and grain boundary mobility. The second class of materials consists of high stacking fault energy metals and alloys. Extensive recovery is expected to take place prior to recrystallization in these materials [36]. Consequently, the nucleation of recrystallization will be sensitive to the competition between the recovery and mobility terms in Eq. (1). An Al-1% Mg alloy is used to illustrate the application of the model for this class of materials.

3.4.1. Material with a negligible recovery of the stored energy

Cu and its alloys have a low to medium stacking fault energy. It is generally observed that very little recovery takes place prior to recrystallization in cold-worked Cu. It is for this reason that the recrystallization kinetics of Cu is frequently studied by means of hardness measurements; the hardness decrease exactly coincides with the onset of recrystallization.

In the absence of recovery, our model can be simplified to derive an analytical expression for the recrystallization incubation time. Assuming that the stored energy does not change with time, we obtain for the appearance of the first nucleus:

$$\Delta t = \frac{2\gamma}{MG^2\chi_{\max}} - \frac{r_0}{MG}$$

As for the stored energy, it was estimated from the flow stress, σ, using the relation relating the flow stress to the square root of the dislocation density [23]:

$$G = \frac{1}{2}\frac{(\sigma - \sigma_{\text{yield}})^2}{M_{\text{Taylor}}^2\alpha^2\mu}$$

The agreement between the measured and calculated values (Table 1) is very good, given the uncertainties associated with the experimental values for the mobility and incubation times. The key point here is that the predicted incubation times have both the right magnitude and the right temperature dependence. This lends support to the idea that nucleation, in low/medium stacking fault energy materials, is controlled by the rate of subgrain/cell growth.

The concept of critical strain requires the assumption that a minimum recystallisation fraction is necessary to be able to observe it experimentally. This amounts to a minimum value of $f\langle r\rangle/(D)$ and naturally introduces the grain size dependence of the critical strain. Cigdem [38] reported the critical strain for recrystallization as a function of the

Table 1
Comparison of the measured [37] and predicted [29] recrystallization incubation times in OF–Cu cold drawn to a reduction of 52% and annealed between 270–330°C

Temperature °C	Measured incubation time (min)	Predicted incubation time (min)
270	2.4	2.6
290	5.4	6.0
310	9	15
330	33	39

annealing temperature and the initial grain size. The experimental data is summarized in Table 2. The knowledge of the relation between the strain and the flow stress allows one to estimate the stored energy G. An excellent agreement between the predicted critical strains for different grain sizes and different annealing temperature is obtained, assuming that the sub-boundary mobility is equal to 0.3 of the high angle boundary mobility.

3.4.2. Material with a non negligible recovery of the stored energy

When cold-worked Al–Mg alloys are annealed, significant recovery is observed prior to the onset of recrystallization [33,36]. As such, the nucleation behavior of these alloys is expected to reflect a competition between the decay of stored energy, as a result of recovery, and the increase in the subgrain size, as a result of subgrain growth under the driving force provided by the stored energy. The rate of recovery was measured and modeled for cold deformed Al-2.5% Mg alloys for strains from 0.1 to 3 and annealing temperatures from 160 to 190°C. The experimental constants needed to relate the flow stress to the stored energy in Al–Mg alloys were taken from the investigation of Guyot and Raynaud [39]. The average initial subgrain size was calculated as a function of stress using the empirical relation suggested by Raj and Pharr [40]. An estimate of the high-angle grain boundary mobility is available from the work of Huang and Humphreys [41] on Al-0.9%Mg. The experimental nucleation data which is used to test the model comes from the investigations by Koizumi et al. [42]. In this investigation a cold rolling reduction of 95% was used and the annealing temperature was varied between 225 and 300 °C. Fig. 7 is a reproduction of the recrystallization curves reported by [42]. The recrystallization incubation times predicted by the model [29] for the above conditions are

Table 2
Comparison of the predicted [29] and measured critical strains for the recrystallization of pure Cu for various temperatures and grain sizes [38]

Grain size (μm)	Temperature (°C)	Measured critical strain	Calculated critical strain
100	550	4	4.6
	600	3.5	3.5
	650	2.6	2.8
250	550	5.5	5.8
	600	4.7	4.4
	650	3.6	3.5
600	550	7.2	7.5
	600	6.1	5.6
	650	5.2	4.4

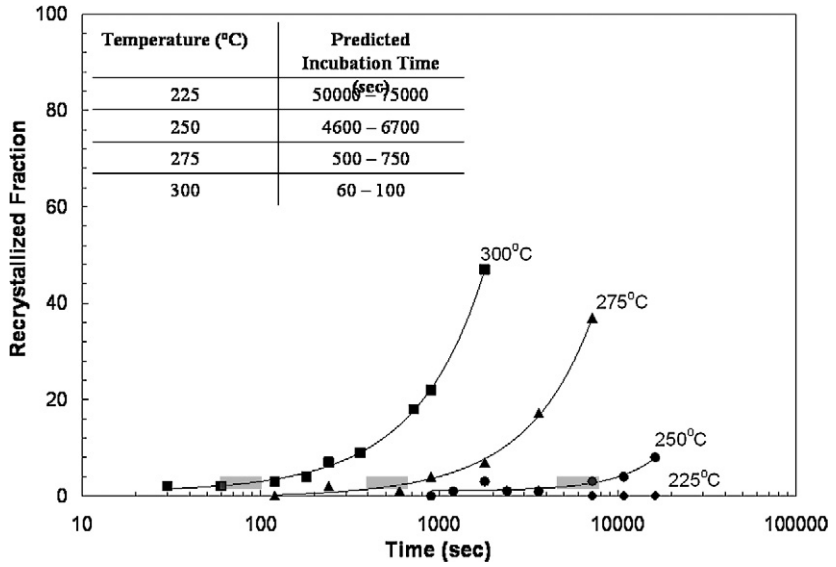

Fig. 7. Recrystallisation kinetics for Al–Mg alloys [42] and predictions for the incubation time [29].

shown in Table 1. These values were calculated for $\chi_{max} = 3$ (lower limit) and $\chi_{max} = 2.5$ (upper limit). In each case the predicted incubation times correspond exactly to the times at which the experimentally measured recrystallized fractions start to increase.

3.5. Conclusions

The simple physically-based model for the nucleation of recrystallization in solid solutions can predict the incubation time, critical strain, critical temperature and nucleation rate of recrystallization. All of the quantities that enter into the model are physically meaningful and measurable. These quantities are: the recovery kinetics, the grain boundary mobility and the initial subgrain size and size distribution. The last two parameters are relatively easy to estimate; extensive tabulations of the subgrain size as a function of deformation exist in the literature and, in most materials, the subgrain size distribution can be approximated by a log normal or a Rayleigh distribution. Concerning the recovery kinetics, it is essential to obtain accurate recovery data when trying to model the nucleation behavior of high stacking fault energy materials. This leaves the boundary mobility as the one input parameter which is hardest to measure reliably, but the key point is that while one may not be able to estimate the boundary mobility exactly, one could at least estimate its temperature dependence which is approximately related to the grain-boundary self-diffusion activation energy. An adjustable parameter could then be introduced into the pre-exponential of the mobility and this could be used to fit the data, as described in the examples of Section 3.4. The present model then provides a one-parameter framework for fitting and rationalizing existing recrystallization data. Once this parameter is established, the model could be used in a predictive manner as long as the elementary nucleation mechanism remains the same. A number of open questions are still pending: what are the recovery kinetics of different texture components? What are the mobilities of boundaries generated in shear bands or transition bands? What is the density of transition bands resulting from given deformation conditions? How can we incorporate misorientation gradients? Misorientation distributions? These issues are central to the developments of predictive models for the final grain size and textures resulting from a given thermomechanical treatment. These features are crucial to understand formability of materials. A number of empirical formulae exist in the literature, the aim of the kind of exercise presented here is to provide for descriptions trying to incorporate as much as possible the mechanisms responsible for the process.

4. Nucleation in the solid state

We stated in the introduction of this article the ubiquity of nucleation processes in physical metallurgy. The two examples treated here show that the use of nucleation words and concepts may be misleading. While nucleation of precipitation is clearly coming from the thermodynamic fluctuations of a supersaturated solid solution, using the same picture (‘adapting’ classical continuum nucleation theory) to recrystallisation is misleading. In recrystallisation, nucleation is to be understood as a structural instability, triggered by the spatial heterogeneities of the dislocation structure and not by fluctuations.

A comparative approach of the two phenomena is enlightening. In precipitation, the species are conserved, while in recrystallisation dislocations are not and do annihilate during recovery. In precipitation, the limiting step is the diffusion of atoms. By contrast, in recrystallisation, the mobility of the interface is a key ingredient, both for the recovery of the subgrain structure, and for the bulging of the grain boundary. In both cases, an incubation time is observed, but for precipitation, it is the time necessary for a stochastic fluctuation of critical size to appear, the latter resulting form atomic scale fluctuations, while for recrystallisation, it is the time necessary to progressively construct in a cumulative manner, a critical configuration.

The basic difference between the two processes stems from the fact that recrystallization is a very far from equilibrium process; unlike precipitation where a mere increase in temperature suffices to revert the process from precipitation to dissolution, there is no way to reversibly change recrystallizing structure into one with a higher dislocation density.

These very different underlying physical phenomena naturally explain the different modelling approaches, and the degree of quantitative modelling: the description of nucleation in precipitation requires inputs at the atomistic level only, and can be made quantitative using appropriate tools from statistical physics. Such tools are not relevant for the nucleation of recrystallisation: the scale of modelling is at the mesoscopic level, and the tools for modelling are much more of the ‘back of the envelope’ type. However, both phenomena illustrate the variety of microstructure

evolution in metals and alloys during thermomechanical treatments, and both require a quantitative modelling both for a fundamental understanding, and from a practical viewpoint, as guides for alloy design.

Acknowledgements

Fruitful collaborations of GM with D. Blavette, E. Clouet, D. Seidman and F. Soisson are gratefully acknowledged. GM was partially supported by an Eshbach Visiting Scholar Award from the McCormick School of Engineering and Applied Science at Northwestern University. Collaboration of YB over the years with P. Guyot, M. Verdier, D. Embury, H. Zurob, C. Hutchinson and J. Dunlop have profoundly influenced the understanding of recrystallisation processes presented here.

References

[1] J. Philibert, Y. Brechet, P. Combrade, A. Vignes, Métallurgie, du minerai au matériau, second ed., Dunod, Paris, 2002.
[2] P. Pareige, B. Radiguet, R. Krummeich-Brangier, A. Barbu, O. Zabusov, M. Kozodaev, Phil. Mag. 85 (2005) 429–441.
[3] A.J. Ardell, Intermetallic compounds as precipitates and dispersoids in high-strength alloys, in: J.H. Westbrook, R.L. Fleischer (Eds.), Intermetallic Compounds: Principles and Practice, vol. 2, John Wiley & Sons, Chichester, England, 1995, pp. 257–286.
[4] L.S. Toropova, D.G. Eskin, M.L. Kharaterova, T.V. Bobatkina, Advanced Aluminum Alloys Containing Scandium—Structure and Properties, Gordon and Breach Sciences, Amsterdam, 1998.
[5] A.R. Allnatt, A.B. Lidiard, Atomic Transport in Solids, Cambridge Univ. Press, Cambridge, UK, 1993.
[6] M. Nastar, V.Yu. Dobretsov, G. Martin, Phil. Mag. A 80 (2000) 155;
M. Nastar, Phil. Mag. 85 (2005) 3767;
V. Barbe, M. Nastar, Phil. Mag. 86 (2006) 1513.
[7] D. Blavette, A. Bostel, J.M. Sarrau, B. Deconihout, A. Menand, Nature 363 (1993) 432.
[8] The main results are being published in: C. Sigli (Ed.), Engineering Materials, in press.
[9] E. Clouet, L. Laë, T. Épicier, W. Lefebvre, M. Nastar, A. Deschamps, Nature Mater. 5 (2006) 482–488.
[10] G. Martin, in: J. Howe, et al. (Eds.), Solid–Solid Phase Transformations in Inorganic Materials, TMS, Warrendale, PA, 2005, pp. 291–299.
[11] E. Clouet, A. Barbu, L. Laë, G. Martin, Acta Mater. 53 (2005) 2313–2325.
[12] A. Perini, G. Jacucci, G. Martin, Phys. Rev. B 29 (1984) 2689.
[13] J. Lepinoux, Phil. Mag. 85 (2005) 3585–3615.
[14] F. Soisson, G. Martin, Phys. Rev. B 62 (2000) 203–214.
[15] Y. Le Bouar, F. Soisson, Phys. Rev. B 65 (2002) 094103.
[16] V. Belova, A.R. Allnatt, G.E. Murch, J. Phys.: Condens. Matter 14 (2002) 6897.
[17] F. Soisson, private communication.
[18] J.M. Roussel, P. Bellon, Phys. Rev. B 63 (2001) 184114.
[19] R. Weinkamer, P. Fratzl, Europhys. Lett. 61 (2003) 261–267.
[20] C. Schmuck, P. Caron, A. Hauet, D. Blavette, Phil. Mag. A 76 (1997) 527–542;
C. Pareige, F. Soisson, G. Martin, D. Blavette, Acta Mater. 47 (1999) 1889–1899.
[21] C.K. Sudbrack, K.E. Yoon, R.D. Noebe, D.N. Seidman, Acta Mater. 54 (2006) 3199–3210.
[22] D. Seidman, et al., in preparation.
[23] J. Friedel, Dislocations, Pergamon Press, Oxford, UK, 1964.
[24] F.J. Humphreys, M. Hatherly, Recrystallization and Related Annealing Phenomena, Pergamon Press, Oxford, UK, 1996.
[25] M. Avrami, J. Chem. Phys. 7 (1939) 1103;
M. Avrami, J. Chem. Phys. 8 (1940) 212;
M. Avrami, J. Chem. Phys. 9 (1941) 117.
[26] C.M. Sellars, in: L. Arnberg, O. Lohne, E. Nes, N. Ryum (Eds.), International Conference on Aluminium Alloys, vol. 3, Trondheim, Norway, 1992, p. 89.
[27] C.M. Sellars, in: N. Hansen, D. Juul-Jensen, T. Leffers, B. Ralph (Eds.), Annealing Processes: Recovery, Recrystallization and Grain Growth, Proceedings of the 7th Riso International Symposium, Riso National Laboratory, Roskilde, Denmark, 1986, p. 167.
[28] J.E. Bailey, P.B. Hirsch, Proc. Royal Soc. A 267 (1962) 11.
[29] H. Zurob, Y. Brechet, J. Dunlop, Acta. Mater. 54 (2006) 3983.
[30] F.J. Humphreys, Acta Mater. 45 (1997) 4231;
F.J. Humphreys, Acta Mater. 45 (1997) 5031;
P.J. Hurley, F.J. Humphreys, Acta Mater. 51 (2003) 3779.
[31] R. Sandstrom, Acta Metall. 25 (1977) 905.
[32] S.K. Varma, Mat. Sci. Engrg. 82 (1986) L19.
[33] M. Verdier, Y. Brechet, P. Guyot, Acta Mater. 47 (1999) 127.
[34] G. Gottstein, L. Shvindlerman, Scripta Metal. 27 (1992) 1515.
[35] O. Kwon, A.J. DeArdo, Acta Metall. Mater. 38 (1990) 41.

[36] E.C.W. Perryman, Trans. AIME 203 (1955) 369;
E.C.W. Perryman, Trans. AIME 205 (1956) 1247;
C. Barioz, Y. Brechet, J.M. Legresy, M.C. Cheynet, in: L. Arnberg, O. Lohne, E. Nes, N. Ryum (Eds.), International Conference on Aluminium Alloys, vol. 2, Trondheim, Norway, 1992, p. 347.
[37] K.P. Haung, W. Form, Z. Metallkd. 80 (1989) 686.
[38] M. Cigdem, Z. Metallkd. 85 (1994) 723.
[39] P. Guyot, G.M. Raynaud, Acta Metall. Mater. 39 (1991) 317.
[40] S.V. Raj, G.M. Pharr, Mater. Sci. Engrg. A 81 (1986) 217.
[41] Y. Huang, F.J. Humphrey, in: G. Gottstein, A. Molodov (Eds.), Recrystallization and Grain Growth: Proceedings of the First Joint International Conference, vol. 1, Aachen, Germany, Springer-Verlag, Berlin/New York, 2001, p. 645.
[42] M. Koizumi, S. Kohara, H. Inagaki, Z. Metallkd. 91 (2000) 460.